

Optimal Dynamic Basis Trading

Bahman Angoshtari ^{*} Tim Leung [†]

This version: April 22, 2022

Abstract

We study the problem of dynamically trading a futures contract and its underlying asset under a stochastic basis model. We describe the basis evolution by a scaled Brownian bridge, but also incorporate the possibility of non-convergence at maturity. The optimal trading strategies are determined from a utility maximization problem under hyperbolic absolute risk aversion (HARA) risk preferences. By analyzing the associated Hamilton-Jacobi-Bellman equation, we derive the exact conditions under which the equation admits a solution and solve the utility maximization explicitly. A series of numerical examples are provided to illustrate the optimal strategies and examine the effects of model parameters.

keywords: futures, stochastic basis, cash and carry, scaled Brownian bridge, risk aversion.

1 Introduction

Basis trading, also known as *cash-and-carry* trading in the context of futures contracts, is a core strategy for many speculative traders who seek to profit from anticipated convergence of spot and futures prices. The practice usually involves taking a long position in the under-priced asset and a short position in the over-priced one, and closing the positions when convergence occurs. In reality, however, basis trading is far from a riskless arbitrage. Unexpected changes in market factors such as interest rate, cost of carry, or dividends can diminish profitability. Moreover, market frictions, such as transaction costs and collateral payments, can turn seemingly certain arbitrage opportunities into disastrous trades. It is also possible that the basis does not converge at maturity. This non-convergence phenomenon was commonly observed in the grains markets. As reported in [Irwin et al. \(2011\)](#), [Adjemian et al. \(2013\)](#), and [Garcia et al. \(2015\)](#), for most of 2005-2010 futures contracts expired up to 35% above the spot price. As a result, some cash-and-carry traders may choose to close their positions prior to maturity to limit risk exposure.

Early works on pricing of futures contracts, such as [Cox et al. \(1981\)](#) and [Modest and Sundaresan \(1983\)](#), established no-arbitrage relationships between the spot price and associated futures prices. Assuming imperfections, such as transaction cost, these relationships take the form of pricing bounds, which can be used for identifying profitable trades. Among related studies on basis trading, [Brennan and Schwartz \(1988\)](#) and [Brennan and Schwartz \(1990\)](#) assumed that the basis of an index futures follows a scaled Brownian

^{*}Department of Applied Mathematics, University of Washington, Seattle WA 98195. e-mail: bahmang@uw.edu

[†]Department of Applied Mathematics, University of Washington, Seattle WA 98195. e-mail: timleung@uw.edu

bridge and that trading the assets is subject to position limits and transaction costs. They calculated the value of the embedded timing options to trade the basis, and used the option prices to devise open-hold-close strategies involving the index futures and the underlying index. Also under a Brownian bridge model, [Dai et al. \(2011\)](#) provided an alternative strategy and specification of transaction costs. Another related work by [Liu and Longstaff \(2004\)](#) assumed that the basis follows a scaled Brownian bridge and the investor is subject to a collateral constraint. They derived the closed-form strategy that maximizes the expected logarithmic utility of terminal wealth, and showed the optimality of taking smaller arbitrage positions well within the collateral constraint.

In the aforementioned studies on optimal basis trading, the market model contains arbitrage. Indeed, it is assumed that the basis, which is a tradable asset, converges to zero at a fixed future time. In this paper, we consider a different scenario where the basis “almost” converges at a fixed future time. More precisely, we model the basis by a scaled Brownian bridge which is stopped before its complete convergence. Our motivation stems from (i) non-convergence of basis, and (ii) a scenario in which the trader stops the trade before convergence occurs. In addition, we show that our model generates an arbitrage-free futures market (see [Proposition 2.4](#)).

We consider a general class of risk preferences by using hyperbolic absolute risk aversion (HARA) utility functions. This family includes common utility functions such as power and exponential utilities, as well as many others. Among our findings, we derive in closed form the optimal dynamic basis trading strategy maximizing the expected utility of terminal wealth. In solving our portfolio optimization problem, the critical question of well-posedness arises. To that end, we find the exact conditions under which the maximum expected utility is finite. For the case where the expected utility explodes, we derive the critical investment horizon at which the explosion happens. See [Section 3](#) for further details. Note that achieving infinite expected utility has been observed in the following contexts: infinite horizon portfolio optimization ([Merton \(1969\)](#)), optimal execution ([Bulthuis et al. \(2017\)](#)), and finite horizon optimal trading of assets with mean-reverting return ([Kim and Omberg \(1996\)](#); [Korn and Kraft \(2004\)](#)). The latter studies, respectively, have coined the terms “*nirvana strategies*” and “*I-unstable*” for investment strategies that yield infinite expected utility in finite investment horizon.

Our model is related to a number of studies in finance involving Brownian bridges. Applications include modeling the flow of information in the market. For example, [Brody, Hughston, and Macrina \(2008\)](#) used a Brownian bridge as the noise in the information about a future market event, and derived option pricing formulae based on this asset price dynamics and market information flow. [Cartea, Jaimungal, and Kinzebulatov \(2016\)](#) utilized a randomized Brownian bridge (rBb) to model the mid-price of an asset with a random end-point perceived by an informed trader, and determined the optimal placements of market and limit orders. [Leung, Li, and Li \(2018\)](#) also applied a rBb model to investigate the optimal timing to sell different option positions.

Basis trading involves trading a single futures contract along with its spot asset. A similar alternative strategy is to trade multiple futures with the spot but different maturities. For instance, [Leung and Yan \(2018\)](#) considered futures prices generated from the same two-factor stochastic spot model and optimize dynamic trading strategies. In optimal convergence trading, asset prices or their spreads are often modeled

by a stationary mean-reverting process. See, for example, [Kim and Omberg \(1996\)](#), [Korn and Kraft \(2004\)](#), [Mudchanatongsuk et al. \(2008\)](#), [Chiu and Wong \(2011\)](#), [Liu and Timmermann \(2013\)](#), [Tourin and Yan \(2013\)](#), [Cartea and Jaimungal \(2016\)](#), [Lee and Papanicolaou \(2016\)](#), [Leung and Li \(2016\)](#), [Kitapbayev and Leung \(2018\)](#), and [Cartea et al. \(2018\)](#). In these studies, however, prices or spreads are not scheduled to converge at a future time. Using a scaled Brownian bridge, we can control the basis's tendency to converge towards the expiration date.

The rest of the paper is organized as follows. In [Section 2](#), we introduce our market model and formulate the dynamic basis trading problem. In [Section 3](#), we solve the associated Hamilton-Jacobi-Bellman partial differential equation. [Section 4](#) contains our results on the optimal basis trading strategy, along with a series of illustrative numerical examples. [Section 5](#) concludes. Longer proofs are included in the Appendix.

2 Problem setup

We consider an investor who trades a riskless asset, a futures contract F with maturity T and its underlying asset S , over a period $[0, T]$. For simplicity, we assume that S does not pay dividends and has no storage cost. We also assume that the interest rate is zero, by taking the riskless asset as the numeraire. Under these assumptions, the futures price, the forward price, and the spot price should be equal. In practice, however, market frictions and inefficiencies may render futures price different from the spot or forward price. As discussed above, the futures price may not even converge to the spot price at maturity.

Motivated by these market imperfections, we propose a stochastic model that incorporates the comovements of the futures and spot prices, and captures the tendency of the basis to approach zero but not necessarily vanish at maturity. In essence, the spot and futures prices are driven by correlated Brownian motions and the stochastic basis is represented by scaled Brownian bridge, as we will show in [Lemma 2.2](#) below.

To describe our model, we assume that the volatility normalized¹ futures price $(F_t)_{t \in [0, T]}$ and the volatility normalized spot price $(S_t)_{t \in [0, T]}$ satisfy

$$\frac{dS_t}{S_t} = \mu_1 dt + dW_{t,1}, \quad (2.1)$$

and

$$\frac{dF_t}{F_t} = \left(\mu_2 + \frac{\kappa Z_t}{T-t+\varepsilon} \right) dt + \rho dW_{t,1} + \sqrt{1-\rho^2} dW_{t,2}, \quad (2.2)$$

where $(Z_t)_{0 \leq t \leq T}$ is the log-value of the stochastic *basis* defined by

$$Z_t := \log \left(\frac{S_t}{F_t} \right); \quad 0 \leq t \leq T. \quad (2.3)$$

Here, $\mathbf{W}_t = (W_{t,1}, W_{t,2})^\top$ is a standard Brownian motion in a filtered probability space $(\Omega, \mathcal{F}, \mathbb{P}, (\mathcal{F}_t)_{t \geq 0})$ where $(\mathcal{F}_t)_{t \geq 0}$ is generated by the Brownian motion and satisfies the usual conditions. The parameters, μ_1 and μ_2 , with $\mu_1, \mu_2 \in \mathbb{R}$, represent the Sharpe ratios of S and F respectively (see [Remark 2.1](#) below). As

¹See [Remark 2.1](#).

specified in (2.2), the futures price has the tendency to revert around S . Indeed, if F_t is significantly higher than S_t , then Z_t becomes negative. Consequently, the drift of F_t can also be negative, and thus driving the value of F_t downward to be closer to S_t . The opposite will hold if F_t is significantly lower than S_t . The speed of this mean reversion is reflected by the constant $\kappa > 0$. On the other hand, the two prices need not coincide at maturity. The level of non-convergence is controlled by the parameter $\varepsilon > 0$. A smaller ε means that at maturity S_T and F_T tend to be closer. In fact, if $\varepsilon = 0$, S_T and F_T will be exactly the same. Lastly, we incorporate correlation between the two price processes through the parameter $|\rho| < 1$.

Remark 2.1. Let (\tilde{S}_t) satisfying

$$d\tilde{S}_t = \tilde{S}_t(\mu_t dt + \sigma_t dW_t),$$

be the quoted price of an asset. The “volatility normalized price” of the asset (S_t) is given by

$$dS_t = \frac{S_t}{\sigma_t \tilde{S}_t} d\tilde{S}_t = S_t \left(\frac{\mu_t}{\sigma_t} dt + dW_t \right), \quad S_0 = \tilde{S}_0,$$

such that the volatility of (S_t) is 1.

Furthermore, let $(\tilde{\pi}_t)$ be the amount invested in the asset. The “volatility adjusted position” in asset S is given by $\pi_t := \sigma_t \tilde{\pi}_t$ such that

$$d\tilde{\pi}_t = \tilde{\pi}_t \frac{d\tilde{S}_t}{\tilde{S}_t} = \pi_t \frac{dS_t}{S_t}.$$

In other words, when working with volatility normalized prices, volatility adjusted positions should be used. To find the \$ positions, we only need to divide the volatility adjusted positions by volatility, i.e. $\tilde{\pi}_t = \frac{\pi_t}{\sigma_t}$.

For the rest of the article, we use the terms prices and positions in place of volatility normalized prices and volatility adjusted positions.

As we show in the following lemma, the price dynamics (2.1) and (2.2) imply that the stochastic basis (Z_t) is a scaled Brownian bridge that converges to zero at $T + \varepsilon$. This implies that S and F converge at $T + \varepsilon$, i.e. $\lim_{t \rightarrow T + \varepsilon} (F_t/S_t) = 1$, \mathbb{P} -almost surely. However, since the futures contract expires at T and $T + \varepsilon$ is past maturity, such a convergence is not realized in the market. In a limiting case of our model where $\varepsilon \rightarrow 0^+$, the spot and future prices converge at T and the market model admits arbitrage. In contrast, for any $\varepsilon > 0$, the market is arbitrage-free. See Proposition 2.4 and Remark 2.5 below.

Lemma 2.2. *The stochastic basis $(Z_t)_{0 \leq t \leq T}$ satisfies*

$$dZ_t = \mu_1 - \mu_2 - \frac{\kappa Z_t}{T - t + \varepsilon} dt + (1 - \rho) dW_{t,1} - \sqrt{1 - \rho^2} dW_{t,2}, \quad (2.4)$$

for $0 \leq t \leq T$. In particular, if we consider the solution of this SDE over $[0, T + \varepsilon]$, then $Z_{T + \varepsilon} = 0$, \mathbb{P} -almost surely.

Proof. We obtain (2.4) by applying (2.1)-(2.3) to $dZ_t = \frac{dS_t}{S_t} - \frac{dF_t}{F_t}$. By Eq. (6.6) on page 354 of Karatzas and Shreve (1991), the unique strong solution of (2.4) is

$$\begin{aligned} Z_t = & Z_0 \left(1 - \frac{t}{T + \varepsilon} \right)^\kappa + (\mu_1 - \mu_2) A(t) \\ & + \int_0^t \left(\frac{T - t + \varepsilon}{T - u + \varepsilon} \right)^\kappa \left((1 - \rho) dW_{u,1} - \sqrt{1 - \rho^2} dW_{u,2} \right); \quad 0 \leq t \leq T, \end{aligned} \quad (2.5)$$

where we have defined

$$A(t) := \begin{cases} \frac{1}{\kappa-1} \left(T-t+\varepsilon - \frac{(T-t+\varepsilon)^\kappa}{(T+\varepsilon)^{\kappa-1}} \right); & \text{if } \kappa \neq 1, \\ (T-t+\varepsilon) \log \left(\frac{T+\varepsilon}{T-t+\varepsilon} \right); & \text{if } \kappa = 1. \end{cases} \quad (2.6)$$

Since $\kappa > 0$, taking limits in (2.6) yields $\lim_{t \rightarrow T+\varepsilon} A(t) = 0$. From (2.5), it follows that $\mathbb{P}(Z_{T+\varepsilon} = 0) = 1$. \square

As a corollary, we now describe the distribution of the basis $(Z_t)_{t \geq 0}$.

Corollary 2.3. *Assume that Z_0 is deterministic. Then, the basis $(Z_t)_{0 \leq t \leq T}$ is a Gauss-Markov process with mean function*

$$m(t) := \mathbb{E}(Z_t) = Z_0 \left(1 - \frac{t}{T+\varepsilon} \right)^\kappa + (\mu_1 - \mu_2)A(t), \quad (2.7)$$

and covariance function

$$\sigma(s, t) := \text{Cov}(Z_s, Z_t) = \begin{cases} \frac{2(1-\rho)}{2\kappa-1} \frac{(T-t+\varepsilon)^\kappa}{(T-s+\varepsilon)^{\kappa-1}} \left(1 - \left(1 - \frac{s}{T+\varepsilon} \right)^{2\kappa-1} \right); & \text{if } \kappa \neq \frac{1}{2}, \\ 2(1-\rho) \sqrt{(T-t+\varepsilon)(T-s+\varepsilon)} \log \left(\frac{T+\varepsilon}{T-s+\varepsilon} \right); & \text{if } \kappa = \frac{1}{2}, \end{cases} \quad (2.8)$$

for all $0 < s \leq t < T$. Here, $A(t)$ is given by (2.6).

Proof. This result follows from direction calculations using (2.5). \square

From Corollary 2.3, it follows that $Z_T \sim N(m(T), \gamma(T, T))$. Furthermore, as $\varepsilon \rightarrow 0$, we have $\mathbb{E}(Z_T) = m(T) \rightarrow 0$ and $\text{Var}(Z_T) = \sigma(T, T) \rightarrow 0$. Using Lemma 2.2 and its corollary, it is straightforward to devise a time-discretization scheme to simulate the paths of S , F , and Z , as shown in Figure 1. As a confirmation, we see the empirical density of Z_T based on 200 simulated paths closely matching with the theoretical density, i.e. $N(m(T), \sigma(T, T))$.

Next, we prove that our market model is arbitrage-free. Let us first define the *market price of risk* function

$$\lambda(t, z) := \Sigma^{-1} \begin{pmatrix} \mu_1 \\ \mu_2 + \frac{\kappa z}{T-t+\varepsilon} \end{pmatrix}; \quad 0 \leq t \leq T,$$

where

$$\Sigma := \begin{pmatrix} 1 & 0 \\ \rho & \sqrt{1-\rho^2} \end{pmatrix}.$$

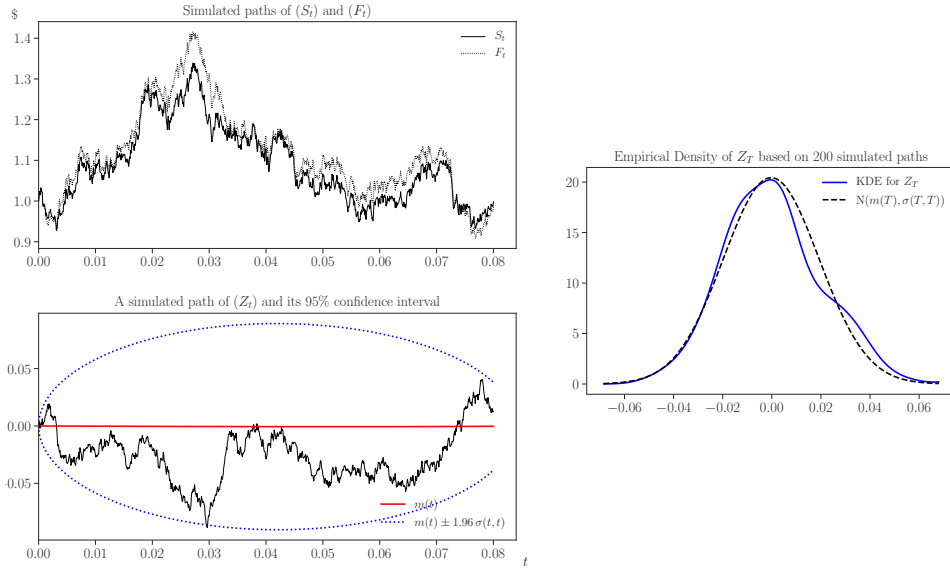


Figure 1: The left panel shows the simulated paths of S and F (top), as well as Z and its confidence interval over time (bottom). On the right, the theoretical and estimated (based on simulated paths) densities of Z_T are plotted. Parameters: $\mu_1 = 0.1$, $\mu_2 = 0.12$, $\kappa = 1$, $T = 0.08$, $\varepsilon = 0.004$, $\rho = 0.95$.

Proposition 2.4. *The market model in (2.1)–(2.3) is arbitrage-free. In particular, the risk-neutral measure \mathbb{Q} is given by the Radon-Nikodym derivative $\frac{d\mathbb{Q}}{d\mathbb{P}} = \zeta_T$, where the process $(\zeta_t)_{t \in [0, T]}$ satisfies*

$$\begin{cases} \frac{d\zeta_t}{\zeta_t} = -\lambda(t, Z_t)^\top d\mathbf{W}_t; & 0 \leq t \leq T, \\ \zeta_0 = 1, \end{cases}$$

and is a \mathbb{P} -martingale.

Proof. See Appendix A. □

Proposition 2.4 shows the importance of having $\varepsilon > 0$. For $\varepsilon = 0$, the market model (2.1)–(2.2) is not arbitrage-free. Indeed, setting $\varepsilon = 0$ in the proof of Lemma 2.2 yields that $\mathbb{P}(S_T = F_T) = \mathbb{P}(Z_T = 0) = 1$. Therefore, if there is a risk-neutral measure \mathbb{Q} , then we must have

$$S_t = \mathbb{E}^{\mathbb{Q}}(S_T) = \mathbb{E}^{\mathbb{Q}}(F_T) = F_t; \quad 0 \leq t \leq T,$$

which contradicts (2.1)–(2.2).

Remark 2.5. With reference to the proof of Proposition 2.4 in Appendix A, we can point out which part would fail if $\varepsilon = 0$. Specifically, for $\varepsilon = 0$, the integral in (A.2), namely

$$\int_0^T \left(\frac{2|\boldsymbol{\mu}^\top \Omega^{-1} \boldsymbol{\eta}|}{T-t} |Z_t| + \frac{\boldsymbol{\eta}^\top \Omega^{-1} \boldsymbol{\eta}}{(T-t)^2} Z_t^2 \right) dt,$$

is divergent, violating the key inequality (A.1) in the proof.

We now discuss the dynamic trading problem faced by the investor. Let $\tilde{\pi}_{t,1}$ be the cash amount invested in S, and $\tilde{\pi}_{t,2}$ the notional value² invested in F, for $t \in [0, T]$. Define the volatility adjusted positions³ by $\pi_{t,i} := \sigma_{t,i} \tilde{\pi}_{t,i}$, $i \in \{1, 2\}$, where $(\sigma_{1,t})$ and $(\sigma_{2,t})$ are the volatilities of the spot and futures prices, respectively. Then, the trading wealth $(X_t)_{0 \leq t \leq T}$ follows

$$\begin{aligned} dX_t &= \pi_{t,1} \frac{dS_t}{S_t} + \pi_{t,2} \frac{dF_t}{F_t} \\ &= \left(\mu_1 \pi_{t,1} + \left(\mu_2 + \frac{\kappa Z_t}{T-t+\varepsilon} \right) \pi_{t,2} \right) dt \\ &\quad + (\pi_{t,1} + \rho \pi_{t,2}) dW_{t,1} + \pi_{t,2} \sqrt{1-\rho^2} dW_{t,2}, \end{aligned} \quad (2.9)$$

for $0 \leq t \leq T$, and with $X_0 = x$.

Next, we define the set of *admissible trading strategies*.

Definition 2.6. For constants $x^*, \gamma \in \mathbb{R}$, define the set $\mathcal{D} \subseteq \mathbb{R}$ as follows

$$\mathcal{D} := \begin{cases} \{x \in \mathbb{R} : x > x^*\}; & \gamma > 0, \\ \{x \in \mathbb{R} : x < x^*\}; & \gamma < 0, \\ \mathbb{R}; & \gamma = 0. \end{cases}$$

We denote by $\mathcal{A} = \mathcal{A}(x^*, \gamma)$ the set of all (\mathcal{F}_t) -adapted processes, denoted by $\pi = (\pi_t^1, \pi_t^2)_{0 \leq t \leq T}$, such that

- (i) $\int_0^T (\pi_{t,1}^2 + \pi_{t,2}^2 + |\pi_{t,2} Z_t|) dt < \infty$, P-a.s.,
- (ii) $X_t \in \mathcal{D}$ P-a.s. for all $t \in [0, T]$, where $(X_t)_{0 \leq t \leq T}$ is given by (2.9),
- (iii) $(X_t)_{0 \leq t \leq T}$ is uniformly bounded from below, P-a.s.

Note that for $\gamma > 0$, Condition (ii) becomes $X_t > x^*$ P-a.s. for all $t \in [0, T]$, which makes Condition (iii) redundant. For $\gamma < 0$, Condition (ii) implies an upper bound on wealth, namely, $X_t < x^*$ P-a.s. for all $t \in [0, T]$. For $\gamma = 0$, Condition (ii) is redundant since the corresponding utility imposes no constraint on the wealth process. Therefore, for $\gamma \leq 0$, Condition (iii) is needed to exclude doubling strategies.

In order to maximize the expected utility of terminal wealth, the investor solves the stochastic control problem

$$V(t, x, z) := \sup_{\pi \in \mathcal{A}} \mathbb{E}_{t,x,z} U(X_T); \quad (t, x, z) \in [0, T] \times \mathcal{D} \times \mathbb{R}, \quad (2.10)$$

where $\mathbb{E}_{t,x,z}(\cdot) := \mathbb{E}(\cdot | X_t = x, Z_t = z)$. Here, $U : \mathcal{D} \rightarrow \mathbb{R}$ is a hyperbolic absolute risk aversion (HARA) utility function whose *risk tolerance* function admits the form:

$$\delta(x) := -\frac{U'(x)}{U''(x)} = \begin{cases} \gamma(x - x^*); & \gamma \neq 0, \\ \delta_0 > 0; & \gamma = 0. \end{cases} \quad (2.11)$$

²That is, the number of futures contracts held multiplied by the futures price.

³See Remark 2.1.

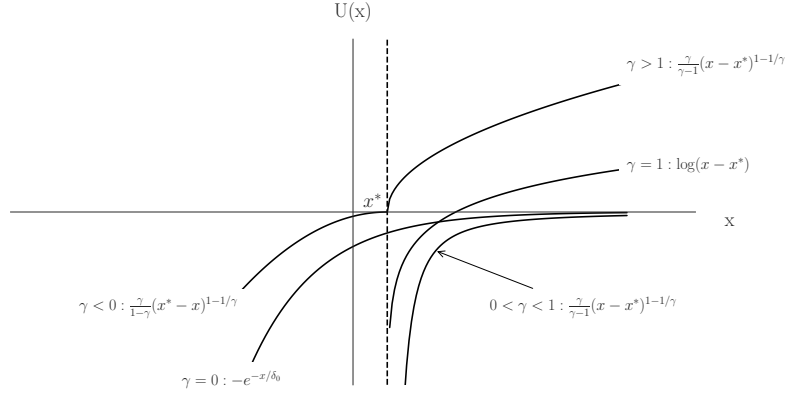


Figure 2: HARA utility functions for different values of γ . Specifically, $\gamma \in (0, 1) \cup (1, \infty)$ yields power utilities, $\gamma = 1$ yields the logarithmic utility, $\gamma = 0$ yields the exponential utility, and $\gamma = -1$ yields the quadratic utility.

We furthermore assume that, for $\gamma \neq 1$,

$$\frac{U(x)}{U'(x)} = \frac{\delta(x)}{\gamma - 1} = \begin{cases} \frac{\gamma}{\gamma - 1}(x - x^*); & \gamma \notin \{0, 1\}, \\ -\delta_0; & \gamma = 0. \end{cases} \quad (2.12)$$

Note that any HARA utility, except the logarithmic utility (i.e. $\gamma = 1$), can be shifted and scaled such that (2.12) is satisfied. Figure 2 illustrates examples of HARA utility functions for different values of γ . Specifically, $\gamma \in (0, 1) \cup (1, \infty)$ corresponds to power utilities, $\gamma = 1$ leads to the logarithmic utility, $\gamma = 0$ yields the exponential utility, and $\gamma = -1$ yields the quadratic utility.

3 HJB equation

As we will show in Section 4, the value function V in (2.10) coincides with the classical solution $v(t, x, z)$ of the following terminal value problem on $[0, T] \times \mathcal{D} \times \mathbb{R}$:

$$\begin{cases} v_t + \left(\mu_1 - \mu_2 - \frac{\kappa z}{T - t + \varepsilon} \right) v_z + (1 - \rho)v_{zz} + \sup_{\pi \in \mathbb{R}^2} \mathcal{L}_\pi v = 0, \\ v(T, x, z) = U(x), \end{cases} \quad (3.1)$$

where the differential operator \mathcal{L}_π is given by

$$\begin{aligned} \mathcal{L}_\pi \varphi(x, z) := & \left(\mu_1 \pi_1 + \left(\mu_2 + \frac{\kappa z}{T - t + \varepsilon} \right) \pi_2 \right) \varphi_x \\ & + \frac{1}{2} \left(\pi_1^2 + \pi_2^2 + 2\pi_1 \pi_2 \rho \right) \varphi_{xx} + (1 - \rho)(\pi_1 - \pi_2) \varphi_{xz}, \end{aligned} \quad (3.2)$$

for any $\pi \in \mathbb{R}^2$ and any function $\varphi(t, x, z)$ with continuous derivatives φ_{xx} and φ_{xz} .

3.1 Well-posedness Conditions

For the rest of this section, we derive the solution for the nonlinear Hamilton-Jacobi-Bellman (HJB) equation (3.1). As it turns out, this equation does not admit a solution for *all* parameter values. This leads us to determine and study the exact conditions under which (3.1) has a solution. To prepare for our results, we define the constant

$$\bar{\gamma} := \frac{\sqrt{2\kappa^2 + (1-2\kappa)(1+\rho)}}{\sqrt{2\kappa(1-\rho)}} - \frac{1-2\kappa+\rho}{2\kappa(1-\rho)} \geq 1.$$

Note that $2\kappa^2 + (1-2\kappa)(1+\rho) = (\kappa-1)^2 + (\kappa-\rho)^2 + \rho(1-\rho) > 0$, and $\bar{\gamma} \geq 1$ since we have assumed that $\kappa > 0$ and $|\rho| < 1$. We now identify the following cases:

- (i) For $\gamma \in (-\infty, 0) \cup (\bar{\gamma}, +\infty)$, (3.1) is “*ill-posed*” in the sense that it has a solution only if $T < T^*(\gamma)$, where $T^*(\gamma)$ is given below.
- (ii) For $\gamma \in [0, 1]$, (3.1) is “*well-posed*” in the sense that it has a unique solution for all values of T .
- (iii) For $\gamma \in (1, \bar{\gamma}]$, (3.1) is “*ill-posed*” (resp. “*well-posed*”) if $0 < \kappa < \frac{1}{2}$ (resp. $\kappa > \frac{1}{2}$). For $\kappa = \frac{1}{2}$, we have $\bar{\gamma} = 1$ and the interval $(1, \bar{\gamma}]$ is empty.

These cases are derived from Theorem 3.3 below.

Achieving infinite expected utility (EU) has been observed in the context of infinite horizon portfolio choice problem (e.g. Merton (1969)), optimal execution (e.g. Bulthuis et al. (2017)), and finite horizon optimal trading of assets with mean-reverting returns (e.g. Kim and Omberg (1996) and Korn and Kraft (2004)). The last two studies, respectively, have coined the terms “*nirvana strategies*” and “*I-unstable*” for investment strategies that yield infinite expected utility over a finite horizon.

In reality, however, investors don’t achieve infinite EU; otherwise they would drive the prices out of equilibrium. This implies that either: (1) there is no investor with risk aversion parameter γ that leads to infinite EU; (2) such an investor exists but the market parameters (that is, κ and ρ) are such that those investors don’t have enough time to achieve infinite EU (i.e. $T < T^*(\gamma)$ for all agents); or (3) market imperfections (such as transaction cost or parameter ambiguity) prevent investors from achieving infinite EU.

3.2 Value Function

Our solution to the HJB equation (3.1) will involve the solution of the following Riccati equation

$$\begin{cases} -h'(t) = 2(1-\rho)\gamma h^2(t) - 2\frac{\gamma\kappa}{T+\varepsilon-t} h(t) - \frac{(1-\gamma)\kappa^2}{(1-\rho^2)(T+\varepsilon-t)^2}, \\ h(T) = 0. \end{cases} \quad (3.3)$$

There is an explicit solution to (3.3), as summarized in Lemma 3.1 below. To prepare for the result, we introduce the following notations. First, define

$$\underline{\gamma} := -\frac{\sqrt{2\kappa^2 + (1-2\kappa)(1+\rho)}}{\sqrt{2\kappa(1-\rho)}} - \frac{1-2\kappa+\rho}{2\kappa(1-\rho)} < 0,$$

and the “discriminant” by

$$\Delta = \Delta(\gamma) := \frac{\rho-1}{\rho+1} \kappa^2 \gamma^2 + \left(\frac{2\kappa}{1+\rho} - 1 \right) \kappa \gamma + \frac{1}{4},$$

Furthermore, we define the “escape time” $T^*(\gamma) \in (0, +\infty]$ as follows:

(i) If $\gamma \in (-\infty, \underline{\gamma}) \cup (\bar{\gamma}, +\infty)$, then

$$T^*(\gamma) = \varepsilon \left[\exp \left(\frac{\pi}{2\sqrt{-\Delta}} - \frac{1}{\sqrt{-\Delta}} \arctan \left(\frac{1-2\gamma\kappa}{2\sqrt{-\Delta}} \right) \right) - 1 \right].$$

(ii) If $\gamma = \underline{\gamma}$, or $\gamma = \bar{\gamma}$ and $0 < \kappa < \frac{1}{2}$, then

$$T^*(\gamma) = \varepsilon \left[\exp \left(\frac{2}{1-2\gamma\kappa} \right) - 1 \right].$$

(iii) If $\gamma \in (\underline{\gamma}, 0)$, or $\gamma \in (1, \bar{\gamma})$ and $0 < \kappa < \frac{1}{2}$, then

$$T^*(\gamma) = \varepsilon \left[\left(\frac{0.5 - \gamma\kappa + \sqrt{\Delta}}{0.5 - \gamma\kappa - \sqrt{\Delta}} \right)^{\frac{1}{2\sqrt{\Delta}}} - 1 \right].$$

(iv) $T^*(\gamma) = +\infty$ for all other values of γ .

The escape time plays a critical role in the Riccati equation.

Lemma 3.1. *The Riccati equation (3.3) has a solution only if $T < T^*(\gamma)$. In particular, if $\gamma \in (-\infty, \underline{\gamma}) \cup (\bar{\gamma}, +\infty)$, then $\Delta(\gamma) < 0$ and the solution is*

$$h(t) = \frac{\sqrt{-\Delta} \tan \left[\sqrt{-\Delta} \log \left(1 + \frac{T-t}{\varepsilon} \right) + \arctan \left(\frac{1-2\gamma\kappa}{2\sqrt{-\Delta}} \right) \right] + \gamma\kappa - \frac{1}{2}}{2\gamma(1-\rho)(T-t+\varepsilon)}.$$

If $\underline{\gamma} \leq \gamma \leq \bar{\gamma}$, then $\Delta(\gamma) \geq 0$ and the solution is

$$h(t) = \begin{cases} -\frac{\kappa^2}{1-\rho^2} \left(\frac{1}{\varepsilon} - \frac{1}{T-t+\varepsilon} \right); & \text{if } \gamma = 0, \\ \left(\frac{\log \left(1 + \frac{T-t}{\varepsilon} \right)}{1 - \left(\frac{1}{2} - \gamma\kappa \right) \log \left(1 + \frac{T-t}{\varepsilon} \right)} \right) \times \left(\frac{\left(\frac{1}{2} - \gamma\kappa \right)^2}{2\gamma(1-\rho)(T-t+\varepsilon)} \right); & \text{if } \gamma = \underline{\gamma}, \bar{\gamma}, \\ \left(\frac{\left(1 + \frac{T-t}{\varepsilon} \right)^{2\sqrt{\Delta}} - 1}{\left(\sqrt{\Delta} - \frac{1}{2} + \gamma\kappa \right) \left(1 + \frac{T-t}{\varepsilon} \right)^{2\sqrt{\Delta}} + \sqrt{\Delta} + \frac{1}{2} - \gamma\kappa} \right) \times \frac{\kappa^2(\gamma-1)}{(1-\rho^2)(T-t+\varepsilon)}; & \text{if } \underline{\gamma} < \gamma < \bar{\gamma}, \gamma \neq 0. \end{cases}$$

If $T^*(\gamma) < +\infty$, then $\lim_{T \rightarrow T^*(\gamma)} |h(0; T)| = +\infty$.

The proof is by direct substitution, and thus omitted.

Remark 3.2. Note that as $\varepsilon \rightarrow 0^+$, we have $T^*(\gamma) \rightarrow 0^+$ for cases (i)-(iii). This is consistent with the scenario where there is arbitrage in the limit $\varepsilon \rightarrow 0^+$.

Now, we present the value function in explicit form.

Theorem 3.3. Assume $T < T^*(\gamma)$. The solution of the HJB equation (3.1) is

$$v(t, x, z) = U(x) \exp \left(f(t) + g(t)z + \frac{1}{2}h(t)z^2 \right), \quad (3.4)$$

for $(t, x, z) \in [0, T] \times \mathcal{D} \times \mathbb{R}$, where $h(t)$ is the solution of (3.3) given by Lemma 3.1, and $g(t)$ and $f(t)$ are given by

$$\begin{cases} g'(t) + \gamma \left(2(1-\rho)h(t) - \frac{\kappa}{T+\varepsilon-t} \right) g(t) \\ \quad = \frac{\kappa(1-\gamma)(\mu_2 - \rho\mu_1)}{(1-\rho^2)(T+\varepsilon-t)} - \gamma(\mu_1 - \mu_2)h(t), \\ g(T) = 0, \end{cases} \quad (3.5)$$

and

$$\begin{aligned} f(t) = & \int_t^T (1-\rho)\gamma g^2(u) + \gamma(\mu_1 - \mu_2)g(u) + (1-\rho)h(u)du \\ & - \frac{(1-\gamma)(\mu_1^2 + \mu_2^2 - 2\rho\mu_2\mu_1)(T-t)}{2(1-\rho^2)}. \end{aligned} \quad (3.6)$$

Proof. See Appendix B. □

Next, we verify that the value function coincides with the solution of the HJB equation (3.1) from Theorem 3.3. We also identify the optimal trading strategy.

Theorem 3.4. Assume $T < T^*(\gamma)$. The value function V in (2.10) is equal to the function v given in Theorem 3.3. Furthermore, the optimal trading strategy, denoted by $\pi^*(t, X_t^*, Z_t)$, is in feedback form, where

$$\begin{aligned} \pi^*(t, x, z) &= \begin{pmatrix} \pi_1^*(t, x, z) \\ \pi_2^*(t, x, z) \end{pmatrix} \\ &= \delta(x) \left[\begin{pmatrix} \frac{\mu_1 - \rho\mu_2}{1-\rho^2} + g(t) \\ \frac{\mu_2 - \rho\mu_1}{1-\rho^2} - g(t) \end{pmatrix} + z \begin{pmatrix} h(t) - \frac{\kappa\rho}{1-\rho^2} \\ -h(t) + \frac{\kappa}{1-\rho^2} \end{pmatrix} \right], \end{aligned} \quad (3.7)$$

for $(t, x, z) \in [0, T] \times \mathcal{D} \times \mathbb{R}$. Here, $\delta(x)$ is the risk tolerance function defined in (2.11).

Proof. See Appendix C. □

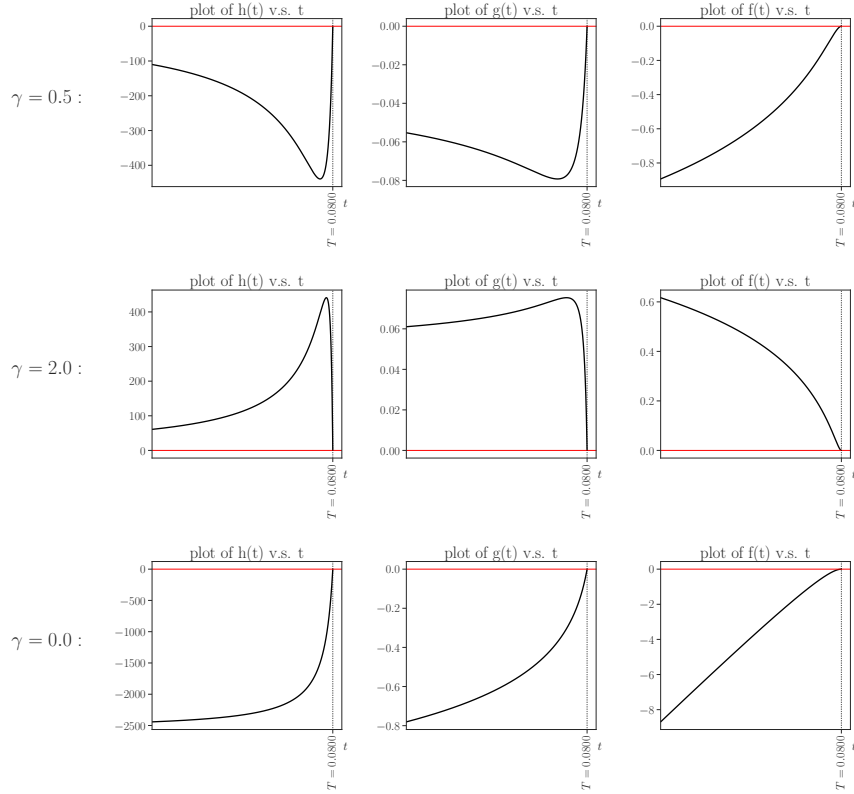


Figure 3: Plots of $h(t)$, $g(t)$, and $f(t)$ for various values of γ in the well-posed range. The model parameters are $\mu_1 = 0.1$, $\mu_2 = 0.12$, $\kappa = 1$, $\varepsilon = 0.004$, $\rho = 0.95$, and $T = 0.08$. The critical values of γ are $\underline{\gamma} = -2.66$ and $\bar{\gamma} = 3.66$.

Figures 3 illustrates the behaviors of functions f , g , and h under three well-posed scenarios. We have set $\kappa = 1$ and $\rho = 0.95$ such that the critical risk aversion values are $\underline{\gamma} = -2.66$ and $\bar{\gamma} = 3.66$. Each row of the figure shows the functions for different value of γ , namely 0, 0.5, and 2. Note that since $\kappa = 1 > 0.5$, the values of γ in the interval $(1, \bar{\gamma} = 3.66)$ are well-posed. In the exponential case (i.e. $\gamma = 0$), h monotonically increases to zero. For the power cases (i.e. $\gamma \in \{0.5, 2\}$), h is not monotone and $|h|$ reaches a maximum of high value before reaching zero. For large values of $T - t$ (i.e. the left end on the x-axis), $h(t)$ seems to flatten. In terms of behaviors, g appears to have similar properties to h , although the values and variations of g is significantly less. In all three scenarios, f moves monotonically to zero over time.

In Figure 4, we consider three ill-posed scenarios. Specifically, we plot $h(t)$ over time for $\gamma > \bar{\gamma}$ (left panel), $\gamma < 0$ (middle panel), and $1 < \gamma < \bar{\gamma}$ and $0 < \kappa < 0.5$ (right panel). In each plot, $h(t)$ is plotted for three choices of T , which are, respectively, 80% (dotted curve), 95% (dashed curve), and 99% (solid curve) of the escape time $T^*(\gamma)$. As expected for these ill-posed cases, we see that $\lim_{T \rightarrow T^*(\gamma)^-} |h(0)| = +\infty$, leading the expected utility to reach the maximum value of the utility function, which is $+\infty$ for $\gamma > 1$ and finite value for $\gamma < 0$, over a finite investment horizon.

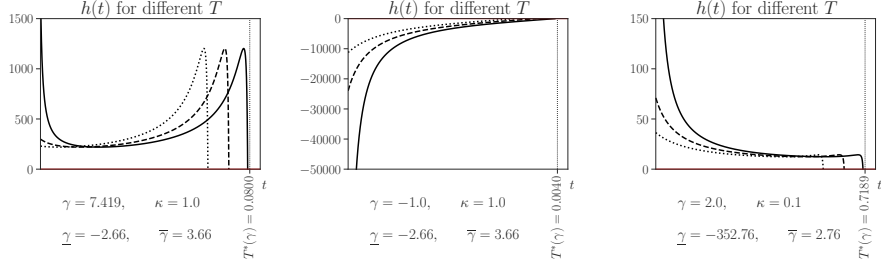


Figure 4: Plots of $h(t)$ for three ill-posed scenarios. In each scenario, three values of T are, respectively, 80% (dotted curve), 95% (dashed curve), and 99% (solid curve) of the escape time $T^*(\gamma)$. The chosen values of γ , κ , $\underline{\gamma}$, and $\bar{\gamma}$ are stated under each plot. The remaining parameters have the same values as in Figure 3.

From Figures 3 and 4, we observe that h is positive for $\gamma > 1$, and negative for $\gamma < 1$.⁴ This motivates us to end the section by showing it analytically. The proof is provided in Appendix.

Lemma 3.5. *Consider $h(t)$, the solution of (3.3), given by Lemma 3.1. If $\gamma < 1$ (resp. $\gamma > 1$), then $h(t) < 0$ (resp. $h(t) > 0$), for all $t \in [0, T]$.*

4 Optimal basis trading strategy

Let us examine the optimal trading strategy π^* in (3.7). Recall from Remark 2.1 that $\pi^*(t, X_t^*, Z_t)$ is the volatility adjusted position. The actual position value is given by $\tilde{\pi}_t = (\frac{\pi_1^*(t, X_t^*, Z_t)}{\sigma_{1,t}}, \frac{\pi_2^*(t, X_t^*, Z_t)}{\sigma_{2,t}})$, where $(\sigma_{1,t})$ and $(\sigma_{2,t})$ are the volatility of the spot and futures prices, respectively.

Our first observation is that π^* is directly proportional to the risk-tolerance function $\delta(x)$. In other words, the larger the risk-tolerance, the larger the optimal positions in (3.7). If we consider the special case with $\kappa = 0$, then it follows that $g \equiv h \equiv 0$, and the optimal strategy π^* reduces to

$$\pi_M := \delta(x) \begin{pmatrix} \frac{\mu_1 - \rho\mu_2}{1 - \rho^2} \\ \frac{\mu_2 - \rho\mu_1}{1 - \rho^2} \end{pmatrix}.$$

This simple strategy does not depend on z . This makes sense because, when $\kappa = 0$, Z_t disappears in the SDE for F_t (see (2.2)). One can loosely interpret π_M as the Merton strategy. More generally, when $\kappa \neq 0$, the incorporation of the scaled Brownian bridge Z_t in F_t makes the optimal strategy π^* dependent on the time varying functions $g(t)$ and $h(t)$ as well as the stochastic factor Z_t .

According to (3.7), for fixed values of x and t , $\pi_1^*(t, x, z)$ and $\pi_2^*(t, x, z)$ are affine functions of z , with the slopes given by $h(t) - \frac{\kappa\rho}{1-\rho^2}$ and $-h(t) + \frac{\kappa}{1-\rho^2}$ respectively. The slope of this function has an interesting interpretation. Note that a positive log basis $Z_t = \log(S_t/F_t)$ means that the spot is priced higher than the futures. To take advantage of the anticipated convergence, our strategy is to take a short position in S and a long position in F. The optimal strategy implies that for larger basis Z_t , the position in S becomes more

⁴Recall that $\gamma = 1$ corresponds to the logarithmic utility which we have excluded from our analysis.

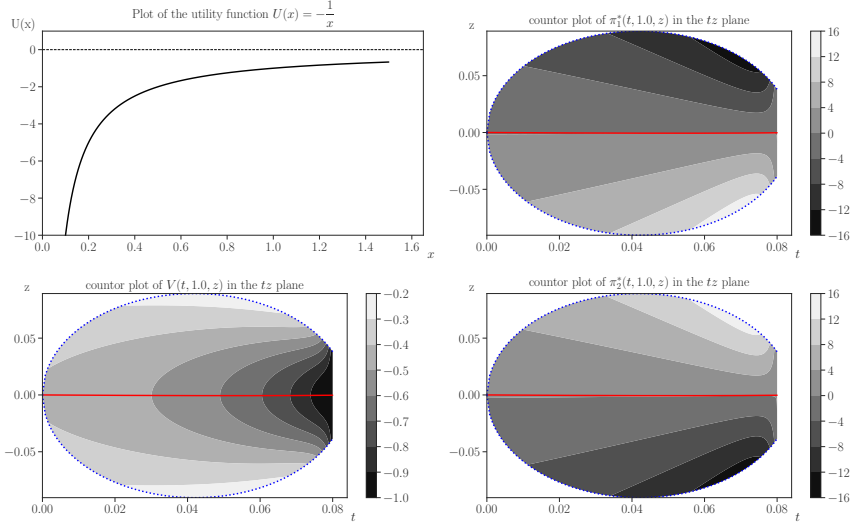


Figure 5: The value function and optimal trading strategy, with the HARA utility function $U(x) = -\frac{1}{x}$ (i.e. $\gamma = 0.5$; top left). Bottom left: contour plot of the value function $V(t, x, z)$ over (t, z) with $x = 1.0$, shaded in the 95% confidence region of (Z_t) , i.e. $\{(t, z) : |z - m(t)| \leq 1.96 * \sigma(t, t)\}$ (see Figure 1). Top and bottom right panels are the respective contour plots of $\pi_1^*(t, 1, z)$ and $\pi_2^*(t, 1, z)$ in the 95% confidence region of (Z_t) .

negative while the position in F becomes more positive. Similarly, for negative values of Z_t (i.e. $F_t > S_t$), one expects to take a short position in F and a long position in S.

For π^* to be a convergence trading strategy, we expect that $h(t) - \frac{\kappa \rho}{1 - \rho^2} \leq 0$ and $-h(t) + \frac{\kappa}{1 - \rho^2} \geq 0$ or, equivalently,

$$h(t) \leq \min\left\{\frac{\kappa \rho}{1 - \rho^2}, \frac{\kappa}{1 - \rho^2}\right\} = \frac{\kappa \rho}{1 - \rho^2}. \quad (4.1)$$

Let's assume that $\rho \geq 0$, that is, the futures and spot prices are non-negatively correlated. Then, (4.1) is always satisfied near maturity, since $\lim_{t \rightarrow T^-} h(t) = 0$. In other words, the optimal strategy always becomes a convergence trading strategy once we are close enough to maturity. It may also be the case that (4.1) is satisfied for all values of $t \in [0, T]$. One sufficient condition is $\gamma \leq 1$ (and $\rho \geq 0$), since Lemma 3.5 yields that $h(t) \leq 0$ for all t . On the other hand, it is also possible for (4.1) to be violated for some parameter values or for t far enough from maturity. We show an example of such a case below.

Figure 5 illustrates the optimal value function and optimal trading strategies for the HARA utility $U(x) = -\frac{1}{x}$ (i.e. $\gamma = 0.5$). Setting $x = 1$, we consider the contour plot of the value function for different values of (t, z) . It is decreasing in t and increasing as z deviates from zero. This is intuitive since a longer time to maturity or larger basis implies more potential for making profits. The 95% confidence region of (Z_t) , i.e. $\{(t, z) : |z - m(t)| \leq 1.96 * \sigma(t, t)\}$, shows that (Z_t) has larger variance near the midpoint of the trading horizon.

The top and bottom right plot of Figure 5 illustrate the optimal positions $\pi_1^*(t, x, z)$ and $\pi_2^*(t, x, z)$ over values of (t, z) in the 95% confidence region. Note that for fixed z and x and as $t \rightarrow T$, position sizes

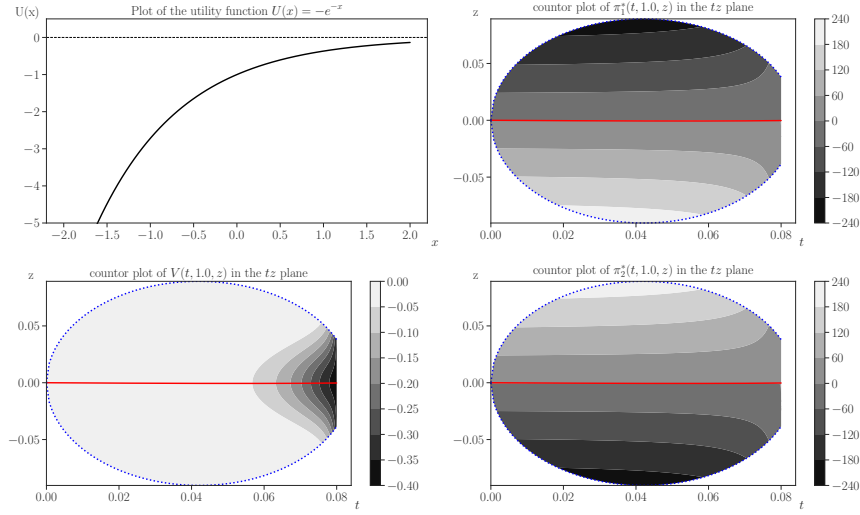


Figure 6: The counterpart of Figure 5 for the exponential utility function $U(x) = -e^{-x}$ (i.e. $\gamma = 0$).

(i.e. $|\pi_i^*(t, x, z)|$, $i = 1, 2$) increase and then decrease. The reason for this behavior can be seen from the corresponding function h in Figure 3, where $|h(t)|$ reached a maximum before vanishing at T . Furthermore, note that for fixed x and t , $\pi_1^*(t, x, z)$ is decreasing in z , while $\pi_2^*(t, x, z)$ is increasing in z . As mentioned above, this is because $h(t) < 0$ and (4.1) is satisfied.

Figure 6 corresponds to the case with exponential utility (i.e. $\gamma = 0$). Note that the value function and optimal positions are much less sensitive to t up till near maturity. Furthermore, the positions appear to change monotonically as time approaches maturity. This is in contrast to the power utility case where position sizes first peak then decrease towards maturity.

In the previous two examples with $\gamma = 0.5$ and $\gamma = 0$, the optimal strategies implies convergence trading in that π_1^* is decreasing and π_2^* is increasing in z . This was expected since $\rho \geq 0$ and $\gamma \leq 1$ and (4.1) was satisfied.

Next, we consider a case where (4.1) does not hold for all values of t . With the utility function $U(x) = 2\sqrt{x}$ (i.e. $\gamma = 2$), the chosen parameter values, $\kappa = 1$ and $\rho = 0.95$, imply that $\frac{\kappa\rho}{1-\rho^2} \approx 9.74$. Thus, $h(t)$ does not satisfy (4.1) (see also Figure 3). From Figure 7, we observe that at time t away from maturity (say, $t = 0.0799$), $\pi_1^*(t, x, z)$ is increasing in z while $\pi_2^*(t, x, z)$ is decreasing. In particular, for large positive values of z , meaning that the spot is higher priced than the futures, it is optimal to long S and short F. This is in contrast to a typical convergence trading strategy. Nevertheless, the optimal strategy from our model eventually becomes convergence trading as time approaches maturity.

Figure 8 illustrates the optimal positions in S and F, along with the corresponding portfolio value, based on the simulated paths and parameters from Figure 1. In this well-posed scenario with $U(x) = -\frac{1}{x}$ ($\gamma = 0.5$), the optimal positions take opposite signs and tend to move in opposite directions. Moreover, whenever the basis Z is negative, the position in S is positive and position in F is negative. The positions are reversed when Z is positive. Furthermore, the optimal positions fluctuate increasingly more rapidly and more sensitive to the basis near maturity.

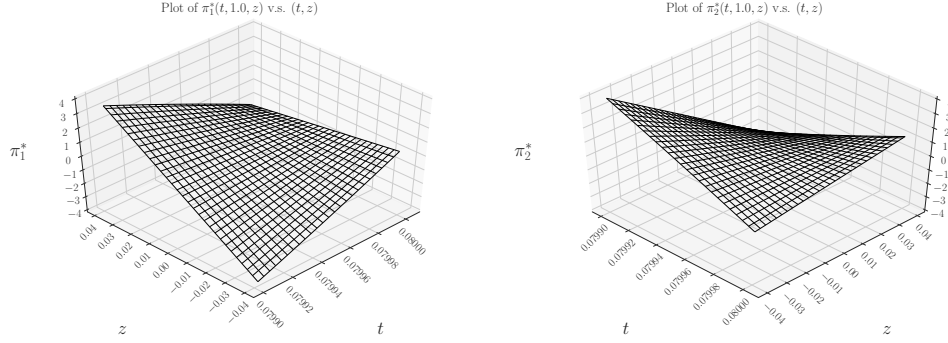


Figure 7: Surface plots of the optimal trading strategies, $\pi_1^*(t, 1, z)$ (left) and $\pi_2^*(t, 1, z)$ (right), for $0.0799 \leq t \leq 0.08 = T$ and $|z - m(t)| \leq 1.96 * \sigma(t, t)$ under the utility $U(x) = 2\sqrt{x}$ ($\gamma = 2$). At time 0.08 (maturity), the strategy trading on convergence in the sense that π_1^* is decreasing in z , while π_2^* is increasing in z . However, at $t = 0.0799$, the strategy is not convergence trading, as π_1^* is increasing in z while π_2^* is decreasing in z .

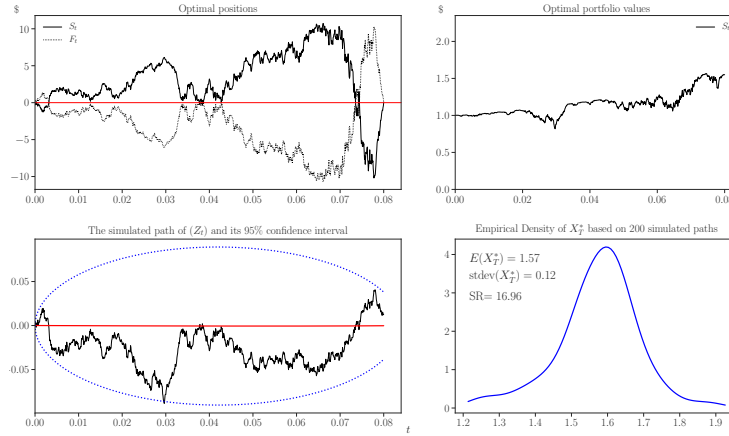


Figure 8: Optimal positions in S and F (top left) for one simulated path of Z (bottom left), with $\gamma = 0.5$ and $x^* = 0$. Top right: the corresponding path of the portfolio value. Bottom right: the empirical density of the optimal terminal wealth X_T^* bases on 200 simulated price paths. Values of other parameters are taken from Figure 1.

In Figure 8 we also see the optimal portfolio value over time. Note that portfolio experience significant drawdowns as Z diverges from equilibrium. This is a common characteristic of convergence trading strategies. The bottom right plot of Figure 8 shows the empirical density of the optimal terminal wealth X_T^* , based on 200 simulated paths. The estimated expected value of terminal wealth is $\mathbb{E}(X_T^*) = 1.57$, with an standard deviation of 0.12. Since the trading horizon is $20/250 = 0.08$ year (i.e. one month), the annualized net expected return is $0.57/0.08 \approx 7.1$ and the annualized volatility is $0.12/\sqrt{0.08} \approx 0.42$. This leads to a Sharpe ratio of $7.1/0.42 \approx 17$ for this simulated example.

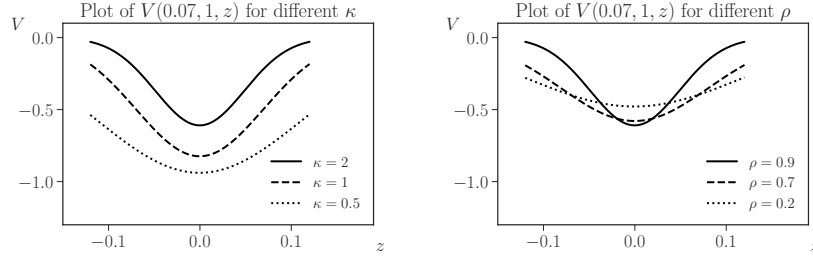


Figure 9: Sensitivity of the value function with respect to κ and ρ . With $t = 0.07$ and $x = 1.0$ fixed, we show $V(0.07, 1, z)$ as a function of z (left) for three values of κ and a fixed value of $\rho = 0.9$, and (right) for three values of ρ with $\kappa = 2$. Other than κ and ρ , parameters values are as in Figure 5.

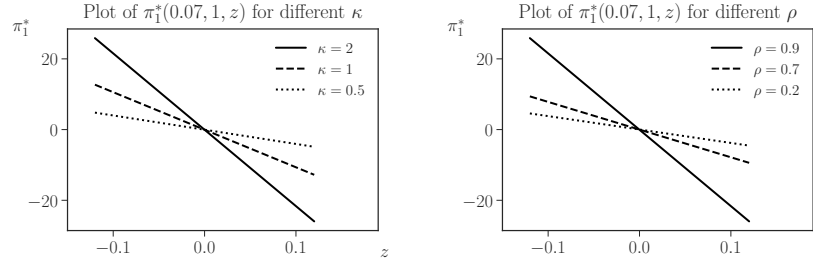


Figure 10: Sensitivity of the optimal spot position with respect to κ and ρ . Setting $t = 0.07$ and $x = 1$, we show $\pi_1^*(0.07, 1, z)$ as a function of basis z (right) for different κ with $\rho = 0.9$, and (right) for different ρ with $\kappa = 2$. A higher mean reversion rate or higher correlation increases the long/short position size when z is negative/positive. Other than κ or ρ , parameters values are the same as in Figure 5.

Turning to the value function, we show in Figure 9 its sensitivity with respect to κ and ρ . For simplicity, we keep $t = 0.07$ and $x = 1.0$ fixed and show $V(0.07, 1, z)$ as a function of z . All other parameters (including the utility function) are as in Figure 5. The value function tends to reach its minimum value at $z = 0$, and a higher κ means a higher value function in the figure. This is intuitive since a higher speed of mean reversion indicates higher profitability from trading the basis at any given level. On correlation increases, the expected utility improves in case of a large mispricing in the assets (i.e. large values of $|z|$) and it decreases when mispricing is small (i.e. for values $|z|$ near zero). This also makes sense. Note that by (2.4), the volatility of the basis (Z_t) is $2(1 - \rho)$, which is decreasing in ρ . Therefore, large correlation indicates less noise in the basis. If there is no mispricing, less noise means less probability of mispricing which lowers the profitability of basis trading. However, if there is a large mispricing, then less noise means that the mispricing will be corrected faster, which increases the profitability and the expected utility.

Figure 10 shows the sensitivity of the optimal spot position with respect to the parameters κ and ρ . For different values of κ and ρ , we see that π_1^* is a decreasing function of z . A higher mean-reversion rate κ or higher correlation ρ makes π_1^* more downward sloping in z , which means that the investor will take a larger long (resp. short) position when z is negative (resp. positive). The financial intuition is as follows.

A higher κ means that the basis tends to converge to zero faster. This represents a more profitable trade, leading the investor to take a larger position in the basis. When the basis is negative, the spot price is below the futures price, so the optimal strategy is to long the spot. The opposite holds when the basis is positive. Increasing ρ decreases the random fluctuations in the basis, which also implies that the basis will show a stronger tendency to converge. Hence, it is optimal to take a larger position.

5 Concluding Remarks

In summary, we have analyzed dynamic trading problem in which a risk-averse investor trades the stochastic basis to maximize expected utility. We describe the non-convergent basis process by a stopped scaled Brownian bridge. This leads us to solve analytically and numerically the associated HJB equation and illustrate the optimal trading strategies.

There are a number of directions for future research. In addition to basis trading, one can analyze other futures trading strategies, including futures rolling, and futures portfolios. Futures are also commonly used in many exchange-traded funds (ETFs) for tracking the spot price (see e.g. [Leung and Ward \(2015\)](#)). It would also be interesting to consider variations of our model. For example, in (2.1) and (2.2), one could interpret that the spot price is instantaneously leading the futures price in that the futures does not have any feedback on the spot. This is a question of price discovery, and we refer to the empirical studies, [Chan \(1992\)](#), [Kawaller et al. \(1987\)](#), and [Stoll and Whaley \(1990\)](#) for more background. It is possible to adapt our solution method by interchanging the leading roles of S and F, and more generally incorporate more sophisticated lead-lag effects between futures and spot prices into the trading problem.

References

- Adjemian, M. K., P. Garcia, S. Irwin, and A. Smith (2013). Non-convergence in domestic commodity futures markets: Causes, consequences, and remedies. *US Department of Agriculture, Economic Research Service 115*, 155381.
- Brennan, M. J. and E. S. Schwartz (1988). Optimal arbitrage strategies under basis variability. In M. Sarnat (Ed.), *Essays in Financial Economics*. North Holland.
- Brennan, M. J. and E. S. Schwartz (1990). Arbitrage in stock index futures. *The Journal of Business* 63(1), S7–S31.
- Brody, D. C., L. P. Hughston, and A. Macrina (2008). Information-based asset pricing. *International Journal of Theoretical and Applied Finance* 11(01), 107–142.
- Bulthuis, B., J. Concha, T. Leung, and B. Ward (2017). Optimal execution of limit and market orders with trade director, speed limiter, and fill uncertainty. *International Journal of Financial Engineering* 4(2-3), 1750020.

- Cartea, Á., L. Gan, and S. Jaimungal (2018). Trading cointegrated assets with price impact. *Mathematical Finance*, Forthcoming 2018, arXiv:1807.01428 [q-fin.TR].
- Cartea, Á. and S. Jaimungal (2016). Algorithmic trading of co-integrated assets. *International Journal of Theoretical and Applied Finance* 19(06), 1650038.
- Cartea, Á., S. Jaimungal, and D. Kinzebulatov (2016). Algorithmic trading with learning. *International Journal of Theoretical and Applied Finance* 19(4), 1650028.
- Chan, K. (1992). A further analysis of the lead-lag relationship between the cash market and stock index futures market. *The Review of Financial Studies* 5(1), 123–152.
- Chiu, M. and H. Wong (2011). Mean-variance portfolio selection of cointegrated assets. *Journal of Economic Dynamics and Control* 35, 1369–1385.
- Cox, J. C., J. F. Ingersoll, and S. A. Ross (1981). The relation between forward and futures price. *Journal of Financial Economics* 9(December), 321–346.
- Dai, M., Y. Zhong, and Y. K. Kwok (2011). Optimal arbitrage strategies on stock index futures under position limits. *Journal of Futures markets* 31(4), 394–406.
- Fleming, W. H. and H. M. Soner (2006). *Controlled Markov Processes and Viscosity Solutions*, Volume 25. Springer New York.
- Garcia, P., S. H. Irwin, and A. Smith (2015). Futures market failure? *American Journal of Agricultural Economics* 97(1), 40–64.
- Irwin, S. H., P. Garcia, D. L. Good, and E. L. Kunda (2011). Spreads and non-convergence in Chicago board of trade corn, soybean, and wheat futures: Are index funds to blame? *Applied Economic Perspectives and Policy* 33(1), 116–142.
- Karatzas, I. and S. Shreve (1991). *Brownian Motion and Stochastic Calculus*. Springer-Verlag.
- Kawaller, I. G., P. D. Koch, and T. W. Koch (1987). The temporal price relationship between S&P 500 futures and the S&P 500 index. *The Journal of Finance* 42(5), 1309–1329.
- Kim, S. and E. Omberg (1996). Dynamic nonmyopic portfolio behavior. *The Review of Financial Studies* 9(1), 141–161.
- Kitapbayev, Y. and T. Leung (2018). Optimal mean-reverting spread trading: Nonlinear integral equation approach. *Annals of Finance* 13(2), 181–203.
- Korn, R. and H. Kraft (2004). On the stability of continuous-time portfolio problems with stochastic opportunity set. *Mathematical Finance* 14(3), 403–414.
- Krylov, N. V. (1980). *Controlled Diffusion Processes*. Applications of Mathematics. Springer.

- Lee, S. and A. Papanicolaou (2016). Pairs trading of two assets with uncertainty in co-integration's level of mean reversion. *International Journal of Theoretical and Applied Finance* 19(08), 1650054.
- Leung, T., J. Li, and X. Li (2018). Optimal timing to trade along a randomized Brownian bridge. *International Journal of Financial Studies* 6(3), 75.
- Leung, T. and X. Li (2016). *Optimal Mean Reversion Trading: Mathematical Analysis And Practical Applications*. World Scientific.
- Leung, T. and B. Ward (2015). The golden target: Analyzing the tracking performance of leveraged gold ETFs. *Studies in Economics and Finance* 32(3), 278–297.
- Leung, T. and R. Yan (2018). Optimal dynamic pairs trading of futures under a two-factor mean-reverting model. *International Journal of Financial Engineering* 5(3), 1850027.
- Liu, J. and F. A. Longstaff (2004). Losing money on arbitrage: Optimal dynamic portfolio choice in markets with arbitrage opportunities. *The Review of Financial Studies* 17(3), 611–641.
- Liu, J. and A. Timmermann (2013). Optimal convergence trade strategies. *Review of Financial Studies* 26(4), 1048–1086.
- Merton, R. C. (1969). Lifetime portfolio selection under uncertainty: The continuous-time case. *Review of Economics and Statistics* 51(3), 247–257.
- Modest, D. M. and M. Sundaresan (1983). The relationship between spot and futures prices in stock index futures markets: Some preliminary evidence. *Journal of Futures Markets* 3(1), 15–41.
- Mudchanatongsuk, S., J. Primbs, and W. Wong (2008). Optimal pairs trading: a stochastic control approach. In *Proceedings of the American Control Conference*, Seattle, Washington, pp. 1035–1039.
- Stoll, H. R. and R. E. Whaley (1990). The dynamics of stock index and stock index futures returns. *Journal of Financial and Quantitative analysis* 25(4), 441–468.
- Tourin, A. and R. Yan (2013). Dynamic pairs trading using the stochastic control approach. *Journal of Economic Dynamics and Control* 37(10), 1972–1981.

A Proof of Proposition 2.4

It suffices to show that \mathbb{Q} is a risk-neutral measure. From (2.1) and (2.2), we have

$$d \begin{pmatrix} S_t \\ F_t \end{pmatrix} = \begin{pmatrix} S_t & 0 \\ 0 & F_t \end{pmatrix} \Sigma (\lambda(t, Z_t) dt + d\mathbf{W}_t); \quad 0 \leq t \leq T.$$

Therefore, by Girsanov's theorem, \mathbb{Q} is a risk-neutral measure if $(\zeta_t)_{0 \leq t \leq T}$ is a \mathbb{P} -martingale. $(\zeta_t)_{0 \leq t \leq T}$ is uniformly integrable (and, thus, a \mathbb{P} -martingale) if

$$\sup_{t \in [0, T]} \mathbb{E} \left| \int_0^t \lambda(u, Z_u)^\top d\mathbf{W}_u \right|^2 < \infty. \quad (\text{A.1})$$

By Corollary 11 of Krylov (1980), there exists a constant $C > 0$, such that

$$\begin{aligned} \sup_{t \in [0, T]} \mathbb{E} \left| \int_0^t \lambda(u, Z_u)^\top d\mathbf{W}_u \right|^2 &\leq C \mathbb{E} \int_0^T \|\lambda(t, Z_t)\|^2 dt \\ &= C \mathbb{E} \left[\boldsymbol{\mu}^\top \Omega^{-1} \boldsymbol{\mu} T + \int_0^T \left(\frac{2|\boldsymbol{\mu}^\top \Omega^{-1} \boldsymbol{\eta}|}{T-t+\varepsilon} |Z_t| + \frac{\boldsymbol{\eta}^\top \Omega^{-1} \boldsymbol{\eta}}{(T-t+\varepsilon)^2} Z_t^2 \right) dt \right], \end{aligned} \quad (\text{A.2})$$

where we have defined

$$\boldsymbol{\mu} := \begin{pmatrix} \mu_1 \\ \mu_2 \end{pmatrix}, \quad \boldsymbol{\eta} := \begin{pmatrix} 0 \\ \kappa \end{pmatrix}, \quad \text{and} \quad \Omega := \Sigma \Sigma^\top = \begin{pmatrix} 1 & \rho \\ \rho & 1 \end{pmatrix}.$$

Therefore, (A.1) holds if $\mathbb{E} \int_0^T Z_t^2 dt < \infty$. Finally, by Fubini's theorem,

$$\mathbb{E} \int_0^T Z_t^2 dt = \int_0^T (\gamma(t, t) + m(t)^2) dt < \infty, \quad (\text{A.3})$$

where $m(t)$ and $\sigma(t, t)$ are bounded functions on $t \in [0, T]$ given by (2.7) and (2.8) respectively.

B Proof of Theorem 3.3

Applying the operator \mathcal{L}_π in (3.2) to the function $v(t, x, z)$ in (3.1), we get

$$\begin{aligned} \mathcal{L}_\pi v(t, x, z) &= \frac{1}{2} v_{xx} \left\| \Sigma^\top \boldsymbol{\pi} + \frac{v_x}{v_{xx}} \Sigma^{-1} \begin{pmatrix} \mu_1 \\ \mu_2 + \frac{\kappa z}{T-t+\varepsilon} \end{pmatrix} + \frac{v_{xz}}{v_{xx}} \Sigma^\top \begin{pmatrix} 1 \\ -1 \end{pmatrix} \right\|^2 \\ &\quad - \frac{1}{2} \left[a \left(\frac{z}{T-t+\varepsilon} \right)^2 + \frac{2b z}{T-t+\varepsilon} + c \right] \frac{v_x^2}{v_{xx}} - (1-\rho) \frac{v_{xz}^2}{v_{xx}} \\ &\quad - \left(\mu_1 - \mu_2 - \frac{\kappa z}{T-t+\varepsilon} \right) \frac{v_x v_{xz}}{v_{xx}}, \end{aligned}$$

where we defined the constants

$$a := \frac{\kappa^2}{1-\rho^2}, \quad b := \frac{\kappa(\mu_2 - \rho\mu_1)}{1-\rho^2}, \quad c := \frac{\mu_1^2 + \mu_2^2 - 2\rho\mu_2\mu_1}{1-\rho^2}, \quad (\text{B.1})$$

and matrix

$$\Sigma := \begin{pmatrix} 1 & 0 \\ \rho & \sqrt{1-\rho^2} \end{pmatrix}.$$

Assume, for now, that $v_{xx}(t, x, z) < 0$, for $(t, x, z) \in [0, T] \times \mathcal{D} \times \mathbb{R}$, which will hold once we show that the solution is of the desired form (3.4). Then, it follows that, for $(t, x, z) \in [0, T] \times \mathcal{D} \times \mathbb{R}$,

$$\begin{aligned} \pi^*(t, x, z) &:= \arg \max_{\pi \in \mathbb{R}^2} \mathcal{L}_\pi v(t, x, z) \\ &= -\frac{v_x}{v_{xx}} (\Sigma \Sigma^\top)^{-1} \begin{pmatrix} \mu_1 \\ \mu_2 + \frac{\kappa z}{T-t+\varepsilon} \end{pmatrix} - \frac{v_{xz}}{v_{xx}} \begin{pmatrix} 1 \\ -1 \end{pmatrix}, \end{aligned} \quad (\text{B.2})$$

and the HJB equation (3.1) becomes to the second-order nonlinear PDE

$$\begin{aligned} v_t(t, x, z) &= \frac{1}{2} \left[a \left(\frac{z}{T-t+\varepsilon} \right)^2 + \frac{2bz}{T-t+\varepsilon} + c \right] \frac{v_x^2}{v_{xx}} \\ &\quad + \left(\mu_1 - \mu_2 - \frac{\kappa z}{T-t+\varepsilon} \right) \left(\frac{v_x v_{xz}}{v_{xx}} - v_z \right) \\ &\quad + (1-\rho) \left(\frac{v_{xz}^2}{v_{xx}} - v_{zz} \right), \end{aligned} \quad (\text{B.3})$$

for $(t, x, z) \in [0, T] \times \mathcal{D} \times \mathbb{R}$ and with the terminal condition $v(T, x, z) = U(x)$. Substituting the ansatz

$$v(t, x, z) = U(x) \exp \left(f(t) + g(t)z + \frac{1}{2}h(t)z^2 \right), \quad (\text{B.4})$$

$(t, x, z) \in [0, T] \times \mathcal{D} \times \mathbb{R}$, in (B.3) leads to the following identity involving the unknown functions f , g , and h ,

$$\begin{aligned} &f'(t) + (1-\rho)\gamma g^2(t) + \gamma(\mu_1 - \mu_2)g(t) + (1-\rho)h(t) - \frac{1}{2}(1-\gamma)c \\ &\quad + z \left[g'(t) + \gamma \left(2(1-\rho)h(t) - \frac{\kappa}{T+\varepsilon-t} \right) g(t) + \gamma(\mu_1 - \mu_2)h(t) - \frac{(1-\gamma)b}{T+\varepsilon-t} \right] \\ &\quad + \frac{1}{2}z^2 \left[h'(t) + 2(1-\rho)\gamma h^2(t) - 2\frac{\gamma\kappa}{T+\varepsilon-t} h(t) - \frac{(1-\gamma)a}{(T+\varepsilon-t)^2} \right] = 0, \end{aligned}$$

for all $t \in [0, T]$ and $z \in \mathbb{R}$. To obtain this equation, we have used the identity

$$\frac{(U'(x))^2}{U''(x)} = (1-\gamma)U(x); \quad x \in \mathcal{D},$$

which follows directly from (2.11) and (2.12). Furthermore, substituting (B.4) in the terminal condition $v(T, x, z) = U(x)$ yields $f(T) = g(T) = h(T) = 0$. As a result, h , g , and f are given by

$$\begin{cases} -h'(t) = 2(1-\rho)\gamma h^2(t) - 2\frac{\gamma\kappa}{T+\varepsilon-t} h(t) - \frac{(1-\gamma)a}{(T+\varepsilon-t)^2}; & t \in [0, T], \\ h(T) = 0, \end{cases} \quad (\text{B.5})$$

$$\begin{cases} g'(t) + \gamma \left(2(1-\rho)h(t) - \frac{\kappa}{T+\varepsilon-t} \right) g(t) \\ \quad + \gamma(\mu_1 - \mu_2)h(t) - \frac{(1-\gamma)b}{T+\varepsilon-t} = 0; & t \in [0, T], \\ g(T) = 0, \end{cases} \quad (\text{B.6})$$

and

$$\begin{cases} -f'(t) = (1-\rho)\gamma g^2(t) + \gamma(\mu_1 - \mu_2)g(t) \\ \quad + (1-\rho)h(t) - \frac{1}{2}(1-\gamma)c; & t \in [0, T], \\ f(T) = 0. \end{cases} \quad (\text{B.7})$$

Note that (B.5) is the Riccati equation (3.3), which we have solved in Lemma 3.1. Now that we obtained h , we can find g using (B.6), and then find f using (B.7). The latter equations yield (3.5) and (3.6) respectively.

C Proof of Theorem 3.4

Let v be the solution of (3.1), given by Theorem 3.3. We prove the following two assertions:

(a) For all $(t, x, z) \in [0, T] \times \mathcal{D} \times \mathbb{R}$, we have

$$v(t, x, z) \geq \mathbb{E}_{t,x,z}(\mathbb{U}(X_T^\pi)), \quad \text{for all } \pi \in \mathcal{A},$$

where X_T^π is the terminal wealth generated by an admissible strategy $\pi \in \mathcal{A}$.

(b) There exists an admissible strategy $\pi^* \in \mathcal{A}_i$ such that the corresponding wealth process $(X_t^*)_{t \in [0, T]}$ satisfies

$$v(t, x, z) = \mathbb{E}_{t,x,z}(\mathbb{U}(X_T^*)); \quad (t, x, z) \in [0, T] \times \mathcal{D} \times \mathbb{R}. \quad (\text{C.1})$$

As a consequence, (a) implies $v \geq V$ and (b) implies $v \leq V$. Hence, if these assertions hold, we obtain $V \equiv v$ as desired.

We consider two cases, namely, $\gamma < 1$ and $\gamma > 1$.

Case 1 ($\gamma < 1$): In this case, by Lemma 3.5, the function h is negative. Therefore, v which is of the form

$$v(t, x, z) = \mathbb{U}(x) \exp\left(f(t) + g(t)z + \frac{1}{2}h(t)z^2\right),$$

is bounded in z . Since v has polynomial growth in x , standard verification results such as Theorem 3.8.1 on page 135 of Fleming and Soner (2006) yield assertions (a) and (b) above. Furthermore, the optimal control is given by (B.2) which, in turn, yields (3.7).

Case 2 ($\gamma > 1$): For these values of γ , Lemma 3.5 shows that h is positive. Thus, v , the solution of the HJB equation, has exponential growth in z . For this case, we provide our own verification result by checking assertions (a) and (b) above.

To show (a), for all $n > 0$, define the stopping times

$$\tau_n := \inf \left\{ t \in (0, T] : \max \left\{ \int_0^t \|\pi_u\|^2 du, |X_t^\pi|, |Z_t| \right\} > n \right\},$$

and note that $\lim_{n \rightarrow +\infty} \tau_n = T$, \mathbb{P} -almost surely. By Itô's formula, we have

$$\begin{aligned} v(t, X_{\tau_n}, Z_{\tau_n}) &= v(t, x, z) \\ &+ \int_t^{\tau_n} \left[v_t(u, X_u, Z_u) + \left(\mu_1 - \mu_2 - \frac{\kappa Z_u}{T-u+\varepsilon} \right) v_z(u, X_u, Z_u) \right. \\ &\quad \left. + (1-\rho)v_{zz}(u, X_u, Z_u) + \mathcal{L}\pi_u v(u, X_u, Z_u) \right] du \\ &+ \int_t^{\tau_n} \left[v_x(u, X_u, Z_u)\pi_u + v_z(u, X_u, Z_u) \begin{pmatrix} 1 \\ -1 \end{pmatrix} \right]^\top \Sigma d\mathbf{W}_u, \end{aligned} \quad (\text{C.2})$$

where Σ is given by (B.1). The first integral on the right side is non-positive because v solves (3.1). Furthermore, by the definition of τ_n , the integrands of the second integral is uniformly bounded, therefore, taking the conditional expectation on both sides of (C.2) yields

$$\mathbb{E}_{t,x,z} v(\tau_n, X_{\tau_n}, Z_{\tau_n}) \leq v(x, z, t). \quad (\text{C.3})$$

Note that for $\gamma > 1$, (2.12) yields that $U > 0$. Thus,

$$v(X_t, Z_t, t) = U(X_t) \exp \left(f(t) + g(t) Z_t + \frac{1}{2} h(t) Z_t^2 \right) > 0.$$

Finally, by letting $n \rightarrow +\infty$, Fatou's lemma yields that $\mathbb{E}_{t,x,z} U(X_T) \leq v(t, x, z)$.

To show (b), define π^* by (3.7), namely,

$$\pi^*(t, x, z) = (x - x^*) \alpha^*(t, z); \quad (t, x, z) \in [0, T] \times \mathcal{D} \times \mathbb{R}, \quad (\text{C.4})$$

where, for ease of notation, we have defined

$$\alpha^*(t, z) := \gamma \left[\begin{pmatrix} \frac{\mu_1 - \rho \mu_2}{1 - \rho^2} + g(t) \\ \frac{\mu_2 - \rho \mu_1}{1 - \rho^2} - g(t) \end{pmatrix} + z \begin{pmatrix} h(t) - \frac{\kappa \rho}{1 - \rho^2} \\ -h(t) + \frac{\kappa}{1 - \rho^2} \end{pmatrix} \right].$$

We need to show that $(\pi^*(t, X_t^*, Z_t))_{t \in [0, T]} \in \mathcal{A}$ and that (C.1) is satisfied.

To show admissibility of $(\pi^*(t, X_t^*, Z_t))_{t \in [0, T]}$, we proceed as follows. By (2.9) and (C.4), the wealth process $(X_t^*)_{t \in [0, T]}$ corresponding to (π_t^*) satisfies

$$\frac{d(X_t^* - x^*)}{X_t^* - x^*} = \alpha^*(t, Z_t)^\top \begin{pmatrix} \mu_1 \\ \mu_2 + \frac{\kappa Z_t}{T-t+\varepsilon} \end{pmatrix} dt + \alpha^*(t, Z_t)^\top \Sigma d\mathbf{W}_t; \quad t \in [0, T].$$

Since $(X_t^* - x^*)_{t \in [0, T]}$ is a stochastic exponential, conditions (i)-(iii) in Definition 2.6 hold if the following integrability condition is satisfied

$$\int_0^T \left(\left\| \alpha^*(t, Z_t)^\top \begin{pmatrix} \mu_1 \\ \mu_2 + \frac{\kappa Z_t}{T-t+\varepsilon} \end{pmatrix} \right\| + \left\| \alpha^*(t, Z_t)^\top \Sigma \right\|^2 \right) dt < \infty; \quad \mathbb{P}\text{-a.s.} \quad (\text{C.5})$$

Since $g(t)$ and $h(t)$ are bounded on the interval $[0, T]$, we have

$$\left\| \alpha^*(t, Z_t)^\top \begin{pmatrix} \mu_1 \\ \mu_2 + \frac{\kappa Z_t}{T-t+\varepsilon} \end{pmatrix} \right\| + \left\| \alpha^*(t, Z_t)^\top \Sigma \right\|^2 < C_1 Z_t^2 + C_2 |Z_t| + C_3, \quad (\text{C.6})$$

for some positive constants C_1 , C_2 , and C_3 . Thus, (C.5) holds if $\int_0^T Z_t^2 dt < \infty$, \mathbb{P} -almost surely. Recall that, by (A.3), $\mathbb{E} \int_0^T Z_t^2 dt < \infty$. It then follows that $\int_0^T Z_t^2 dt < \infty$, \mathbb{P} -a.s. which, along with (C.6), proves that (C.5) holds. We have proved that $(\pi^*(t, X_t^*, Z_t))_{t \in [0, T]} \in \mathcal{A}$.

It only remains to prove (C.1). Since π^* satisfies (B.2), we have

$$v_t + \left(\mu_1 - \mu_2 - \frac{\kappa z}{T - t + \varepsilon} \right) v_z + (1 - \rho) v_{zz} + \mathcal{L}_{\pi^*(t, x, z)} v = 0, \quad (\text{C.7})$$

for $(t, x, z) \in [0, T] \times \mathcal{D} \times \mathbb{R}$. Therefore, by setting $\pi_t = \pi_t^* := \pi^*(t, X_t^*, Z_t)$ in the argument that yielded (C.3), we obtain

$$\mathbb{E}_{t, x, z} v(\tau_n, X_{\tau_n}^*, Z_{\tau_n}) = v(x, z, t); \quad (t, x, z) \in [0, T] \times \mathcal{D} \times \mathbb{R}. \quad (\text{C.8})$$

Next, we show that the process $(v(t, X_t^*, Z_t))_{t \in [0, T]}$ is uniformly integrable. Once we show this, (C.1) follows from (C.8) by taking the limit as $n \rightarrow +\infty$.

Set $\pi_t = \pi_t^*$ in (C.2) and use (C.7) to obtain

$$\begin{aligned} dv(t, X_t^*, Z_t) &= \left[v_x(t, X_t^*, Z_t) \pi_t^* + v_z(t, X_t^*, Z_t) \begin{pmatrix} 1 \\ -1 \end{pmatrix} \right]^\top \Sigma d\mathbf{W}_t \\ &= \left[\frac{v(t, X_t^*, Z_t)}{\frac{\gamma}{\gamma-1}(X_t - x^*)} (X_t^* - x^*) \alpha^*(t, Z_t) \right. \\ &\quad \left. + v(t, X_t^*, Z_t) (g(t) + h(t)Z_t) \begin{pmatrix} 1 \\ -1 \end{pmatrix} \right]^\top \Sigma d\mathbf{W}_t \\ &= v(t, X_t^*, Z_t) \left[\left(1 - \frac{1}{\gamma}\right) \alpha^*(t, Z_t) + (g(t) + h(t)Z_t) \begin{pmatrix} 1 \\ -1 \end{pmatrix} \right]^\top \Sigma d\mathbf{W}_t, \end{aligned}$$

for $t \in [0, T]$. Since $(v(t, X_t^*, Z_t))_{t \in [0, T]}$ is a stochastic exponential, it is uniformly integrable if

$$\sup_{s \in [0, T]} \mathbb{E} \left\| \int_0^s \left[\left(1 - \frac{1}{\gamma}\right) \alpha^*(t, Z_t) + (g(t) + h(t)Z_t) \begin{pmatrix} 1 \\ -1 \end{pmatrix} \right]^\top \Sigma d\mathbf{W}_t \right\|^2 < \infty. \quad (\text{C.9})$$

By Corollary 11 on page 85 of Krylov (1980), there exists a constant $C > 0$ such that

$$\begin{aligned} &\sup_{s \in [0, T]} \mathbb{E} \left\| \int_0^s \left[\left(1 - \frac{1}{\gamma}\right) \alpha^*(t, Z_t) + (g(t) + h(t)Z_t) \begin{pmatrix} 1 \\ -1 \end{pmatrix} \right]^\top \Sigma d\mathbf{W}_t \right\|^2 \\ &\leq C \mathbb{E} \int_0^T \left\| \left[\left(1 - \frac{1}{\gamma}\right) \alpha^*(t, Z_t) + (g(t) + h(t)Z_t) \begin{pmatrix} 1 \\ -1 \end{pmatrix} \right]^\top \Sigma \right\|^2 dt. \end{aligned}$$

Furthermore, since $g(t)$ and $h(t)$ are bounded for $t \in [0, T]$, we have

$$\left\| \left[\left(1 - \frac{1}{\gamma}\right) \alpha^*(t, Z_t) + (g(t) + h(t)Z_t) \begin{pmatrix} 1 \\ -1 \end{pmatrix} \right]^\top \Sigma \right\|^2 \leq K_1 + K_2 |Z_t| + K_3 Z_t^2,$$

for some positive constants K_1 , K_2 , and K_3 . Finally, by (A.3), we have $\mathbb{E} \int_0^T Z_t^2 dt < \infty$ and (C.9) is satisfied.

D Proof of Lemma 3.5

We first show that, for $\gamma > 1$, $h(t) > 0$ for all $t \in [0, T)$. With $\gamma > 1$, ODE (3.3) yields

$$h'(T) = \frac{(1-\gamma)\kappa^2}{\varepsilon^2(1-\rho^2)} < 0.$$

Since $h(T) = 0$, we must have $h(t) > 0$ in a left neighborhood of T , say $t \in [s, T)$ for some $0 \leq s < T$. For $h(t) > 0$ for all $t \in [0, T)$, we show that $h(t) \neq 0$ for all $t \in [0, s)$.

Assume otherwise, that is, $h(t_0) = 0$ for some $t_0 \in [0, s)$. Then, it follows from (3.3) that

$$h'(t_0) = \frac{(1-\gamma)\kappa^2}{(1-\rho^2)(T+\varepsilon-t_0)^2} < 0.$$

This implies that $h(t) < 0$ in a right neighborhood of t_0 , say $t \in (t_0, s']$, for some $s' < s$. Now, since the smooth function h increases from $h(s') < 0$ to $h(s) > 0$ on the interval $[s', s]$, there must be a point $\tau \in (s', s)$ such that $h(\tau) = 0$ and $h'(\tau) \geq 0$. However, by (3.3),

$$h'(\tau) = \frac{(1-\gamma)\kappa^2}{(1-\rho^2)(T+\varepsilon-\tau)^2} < 0,$$

which is a contradiction. Therefore, there cannot be such t_0 , as desired. The proof for the case with $\gamma < 1$ follows from a similar argument and is thus omitted.